


Identification of Eruptive YSOs Within Cygnus-X using NEOWISE Light Curves and the SPICY Catalogue

C. Morris¹ , P. W. Lucas¹, Z. Guo^{2,3,4,1}, N. Miller¹ and C. Contreras-Peña^{5,6}

¹Centre for Astrophysics Research, University of Hertfordshire, College Lane, Hatfield, Hertfordshire, AL10 9AB, UK

²Instituto de Física y Astronomía, Universidad de Valparaíso, ave. Gran Bretaña, 1111, Casilla 5030, Valparaíso, CL

³Núcleo Milenio de Formación Planetaria (NPF), ave. Gran Bretaña, 1111, Casilla 5030, Valparaíso, CL

⁴Departamento de Física, Universidad Técnica Federico Santa María, Avenida España 1680, Valparaíso, Chile

Accepted XXX. Received YYY; in original form ZZZ

ABSTRACT

We have undertaken a thorough examination of the mid-infrared eruptive behaviour of YSOs in the Cygnus-X star-forming region over the last decade, using NEOWISE. The work compares two groups of young stars: embedded class I objects, and the older flat-spectrum and class II sources. We report on 70 eruptive variable candidates within these groups, including 22 with FU Ori-like characteristics. We find the FUor-like stars to be far more commonplace in the younger class I systems, than the older groups, and display colour behaviour that contrasts with stars from the literature. Finally, we note the unusual long-term behaviour of 10 stars, exclusively class I's, that have eruption rise times on the order of 5 or more years. This being far slower than ~6-12 month events for the historical members of this class.

Key words: stars: pre-main sequence – stars: protostar – stars: variables: T Tauri – infrared: stars

1 INTRODUCTION

The long duration time coverage of existing MIR all sky surveys, with Spitzer, WISE and the current NEOWISE (Hora et al. 2007; Wright et al. 2010; Mainzer et al. 2014), provides the ability to find all but the more short-term variable events (such as STVs). The nearby region of Cygnus-X (at roughly 1.4kpc) makes an excellent test site for studying the long-term behaviour of YSOs, because of the wide range of surveys it is included within. These span numerous wavelengths and cover a long time baseline, hence the completeness of YSO candidates in the region is sufficiently high to facilitate in-depth study. The large sample of Kryukova et al. (2014b), which identifies over 2000 candidate YSOs, utilised the full MIR coverage provided by *Spitzer* (from *II* to MIPS [24]) to isolate YSO candidates on the basis of MIR colour, these sources are exclusively Class I YSOs. The same region of sky is also covered by NEOWISE, UGPS (Lucas et al. 2008a), 2MASS (Skrutskie et al. 2006), & IPHAS (Barentsen et al. 2014), as well as being included in the SPICY (Kuhn et al. 2021) catalogue of YSOs.

SPICY uses a mixture of traditional MIR and NIR colour-cuts and random forest classifiers to produce a broadly comprehensive list of YSOs in the 613² deg covered by the existing cryogenic-era glimpse surveys. This selection finds a large number of class II and flat spectrum sources (in addition to Class I's), in this instance there are 7281 additional YSOs, from those found in the aforementioned sample from the Cygnus-X Legacy Survey. Given the broad wavelength coverage of the region, there lies an opportunity to investigate the range and frequency of both high amplitude variability generally and eruptive variability specifically, for YSOs at different ages.

Class I sources are more embedded and brighter in the MIR than most Flat-spectrum (FS) or Class II YSOs, and thus *Spitzer* 24 micron detections can be used to form two distinct samples that can be compared.

Understanding the longer term time-domain behaviour of these systems can be carried out with the post-reactivation NEOWISE survey which covers the whole sky in both the 3.6 μ m W1 & 4.5 μ m W2 bands. At present there has been over 7 years of coverage, with between 2 and 3 epochs per year (depending on the region). Considering the higher MIR brightness of the class I protostars, NEOWISE selection will preferentially target the younger objects. Such a search for EVs at this age range has not been previously carried out.

The incidence rate of eruptive variability in YSOs is subject of importance when considering the 'protostellar luminosity spread problem', but the variance in amplitude (with respect to the photometric bandpasses being used for observations) hasn't been probed in detail previously. Using an unbiased sample of nearby YSOs we can use the NEOWISE data discussed above to examine the range of eruptive behaviours seen in MIR selected YSOs. This should provide insight into how common the usual FUor and EXor (and the more recently uncovered variants thereof) variables are among a MIR selected population, or if other eruptive stars will dominate this feature space.

Whilst variability is common in all YSOs, for the most part this is of low amplitude, and driven by small changes in the disk, accretion rate, or by stellar rotation. Of greater importance are the large accretion bursts primarily of the EX Lupi (EXor) and FU Ori (FUor) types (as well as variations thereof) during which young stars can accrete a significant portion of their final mass (see Hartmann & Kenyon (1996b)). These bursts can have a myriad of differing triggering

* E-mail: c. morris6@herts.ac.uk

mechanisms, with theoretical studies able to reproduce outbursts via: Gravitational Instability (GI) and magnetically driven turbulence in the inner disk (Kratter & Lodato (2016); Bourdarot et al. (2023)), thermal instabilities (Bell & Lin (1994)), disk fragmentation (due to instabilities Vorobyov & Basu (2010) or young massive planets Clarke et al. (2005)) and stellar flybys (Cuello et al. (2019); Borchert et al. (2022b)) to name a selection. This wide range also ensures that there is no universal model for an episodic accretion event, and thus large observationally confirmed samples of these events will be required to understand them further. These methods and other science associated with the mass assembly of young stars can be found in the excellent reviews by Audard et al. (2014); Manara et al. (2022) and references therein.

The FUor type stars are characterised by long-lasting (order of decades) outbursts of high amplitude and a comparatively short brightening time, on the order of ~ 1000 days. These outbursts are considered rare (occurrence timescales are considered to be on the order of 10^5 years (Scholz et al. 2013)), with only a few dozen confirmed with both spectroscopy and photometry (see Connelley & Reipurth (2018) for a range of examples), as well as those identified by VVV and Gaia time series photometry (such as in Contreras Peña et al. (2017) and Hillenbrand et al. (2018)). These outbursts are driven by massively enhanced accretion (the rate can be as high as $10^{-4} M_{\odot} \text{yr}^{-1}$), which will then cause the inner accretion disk to become self-luminous, and outshine the young star's photosphere, hence the distinctive spectrum of these objects (Zhu et al. 2009; Hartmann et al. 2011; Liu et al. 2022). EXors are mostly distinct from FUors, with much shorter outbursts, with durations of between months and a few years, often with similar rise and cooling timescales. There is a broad range of behaviours in the time-domain for EXors, with some near-periodic stars (Guo et al. 2022), some repeating bursters (Kuhn et al. 2023), and others with just single observed event, see Lorenzetti et al. (2012) for further examples. Uniform amongst most EXors however, is that the YSOs maintain magnetospheric accretion (as opposed to the gravitational instability driven accretion in FUors), with spectra frequently containing hydrogen recombination lines. Recently the distinctions between eruptive YSO types have been blurred, with work of Contreras Peña et al. (2017); Guo et al. (2021) using the VVV survey (Minniti et al. 2010), and the recent review by Fischer et al. (2022) noting a much wider array of behaviours and sub-categories. These include the MNor (or V1647 Ori-type), consisting of YSOs with photometric features similar to FUors, but with spectroscopic traits more comparable to EXors. The range of behaviours is further challenged by the authors of Guo et al. (2021) finding that the majority of long-duration outbursts were displaying EXor-like magnetospheric accretion signatures in their spectra.

It has been shown that FUor-like objects more closely resemble Class I and Class 0 protostars than the Class II and flat-spectrum sources that make up a larger number of the observed FUors (see Sandell & Weintraub (2001) or Hartmann & Kenyon (1996a)). It thus stands to reason that these outbursts should be more common at younger ages, and that our current list of known examples is subject so a possibly strong selection bias. This is likely driven by the larger amplitudes observed in the optical and NIR, that will make stars with a less massive envelope easier to detect in outburst, hence improving their number density. Undertaking a more detailed survey of younger system's long term time-domain behaviour, using the MIR, should uncover a large number of long-term eruptive systems, if they are more common at this earlier evolutionary stage.

In this work we will present two selections of YSOs within the region of Cygnus-X: one of embedded objects with a 24 micron de-

tection, mostly Class I YSOs with a small number of flat-spectrum stars. The other is comprised of non-embedded flat-spectrum and class II/III sources (likely without envelopes). Within section 4 we will discuss individual eruptive variables of interest within each selection. Then in section 5 we will compare the incidence of eruptive variability (and of the FUor phenomenon in particular) between both populations, and of similar sources from the literature.

2 SAMPLE SELECTION AND DATA PROCESSING

Starting with the 2007 YSO candidates of Kryukova et al. (2014a), we extracted NEOWISE LCs from the NASA/IPAC IRSA for the 1552 stars with valid detections in both *W1* and *W2*. Of these 1332 had detections in at least 50% of the possible epochs of single scan data.

For each light curve the NEOWISE single-scan data were combined with the earlier ALLWISE measurements (where available). The photometry from the individual scans were then cleaned to remove points with either a high psf error or χ^2 value (> 8), and the median value was calculated for each epoch. We take the error on the mean for the cleaned single-scan images at each epoch, rather than the stated photometric error. This change was motivated by the spread in fluxes at each epoch being larger than the stated errors, which may be indicative of an underlying underestimate of errors in the WISE data. Additional data cleaning involved removing photometric measurements which were associated with quality control flags attributed to the frame itself ('qual_frame' $\neq 0$) or those which had measured fluxes as upper limits only.

To remove any bias associated with selection of more heavily embedded YSOs (as well as investigating the distribution of EVs within this regime), a counterpart sample of sources from SPICY (Kuhn et al. 2021), featuring all candidate YSOs within the sky area used by Kryukova et al. (2014a), that did not feature in those authors sample. the SPICY sample includes 7281 stars, of which 5592 possess NEOWISE light curves, and 4935 have data of sufficient quality for analysis.

The light curves in the first sample were investigated by eye to locate eruptive YSOs. The list of targets for inspection was shortened to include only those targets with peak amplitudes of > 1 mag in either *W1* or *W2*. Candidate FUors were separated from other high amplitude sources through fitting to a characteristic shape, defined by the rising slope, and a burst outburst linear decay. The two component rising slope is defined thus (as listed in Lucas et. al. (Submitted) and Guo et. al. (submitted)):

$$m(t) = m_q - \frac{s}{1 + e^{-(t-t_0)/\tau}} \quad t < t_0$$

$$m(t) = m_q - s(0.5 + 0.25(t - t_0)/\tau) \quad t_0 \leq t \leq t_0 + 2\tau$$

where $m(t)$ is magnitude as a function of time (t), m_q is the magnitude at quiescence, t_0 is the time at which the star is at half the peak amplitude (s), and τ is a metric indicating half of the duration of the accretion burst. The fitting combines the above slope with a linear decay component that runs from 2τ to the end of the time axis. The fit itself makes use of `scipy's curvefit` routine, using the above model, to fit the initial guesses for 5 free parameters (τ , t_0 , m_q , s & the final magnitude), that are then fit by `emcee` over 10000 iterations (this code is now packaged as part of `aptare`¹). The sources with the lowest reduced mean squared error are then inspected to confirm that they are FUor-like.

¹ Available at <https://github.com/nialljmilller/Aptare>

3 ADDITIONAL DATA PRODUCTS

In addition to the NEOWISE light-curves, we also obtained follow-up photometry for (5/10) of the identified EV candidates which were anticipated to be in outburst. For this we were awarded DDT time on the 3.5m telescope at CAHA², using Omega-2000 (Kovács et al. 2004), which is an NIR camera with an $238.7''^2$ FOV situated on the prime focus. Our data consists of *J*, *H*, & *K* band photometry, which can then be combined with archival data to make both pre and post-outburst SEDs.

We also present 3 *K*-band NIR spectra for two of the candidates, which were taken from two sets of observations of suspected eruptive YSOs identified with the UKIDSS survey of high amplitude variable stars (Lucas et al. 2017). Two are from Gemini/NIFS across the summers of 2013 and 2014, and the other being observed with Subaru/IRCS during July 2017. The NIFS spectra were originally part of the PhD thesis of Carlos Contreras-Peña (Contreras Peña 2015).

4 RESULTS

4.1 Stars with MIPS [24] detection

The following selection is majoritively of class I YSOs, with a small number of FS sources (these stars will still have redder SED slopes than is common however, as they must have $[3.6] - [4.5] \geq 0$, as per Kryukova et al. (2014a)). We present the candidate eruptive variables in three groups, corresponding to their long-term MIR behaviour. Section 4.1.1 details the stars with light curve morphologies that most closely resemble the range seen in FUor-type variable stars, although all but one are not listed as FUors directly, as they have not been spectroscopically observed at this juncture. We then discuss a selection of the short-term variables that are EXor-like in their amplitudes and durations (section 4.1.2), although their colour behaviour is rarely the same as in the classical case. Finally in section 4.1.4 we display a selection of candidate eruptive YSOs that are characterised by very long rise times when compared to traditional EVs.

4.1.1 New FUor-like/Long Duration Eruptive YSOs

We identify 6 stars that show FUor-like morphologies, one of which (Source 257) can be considered to be a bona-fide FUor, on the strength that it also has the characteristic spectrum of this type, which can be seen in Contreras-Peña et al. Submitted. This star makes an excellent test case for the other members of this group, with such features as a high (3.28 mag) burst in *W1*, rising over a short time-frame of ~ 2 years, and steadily blueing MIR colours, all being commonly seen in FU Orionis objects.

Of the other stars in this selection, Sources 294 and 1475 are the most similar to Source 257 in their amplitudes, colours and overall durations. Both appear to have a long cooling timescale [zzz fit? zzz], and have peak amplitudes of 2.21 mag and 2.54 mag in *W1* respectively. Neither star has an optical counterpart, and no burst can be seen in monitoring via ZTF (from the forced photometry service), although their *K*-band amplitudes can be found in Table ??.

Source 1999 has the 2nd largest outburst in the sample, but this

is joined by a much steeper cooling slope than the three stars mentioned previously, indicative of a shorter outburst duration than most classical FUors.

The remaining three objects are more distant from the classical FUor morphology, although in the case of Source 2003 that is because the current outburst is yet to finish. We include the source here as a result of the large 5.1 mag *W1* amplitude and the > 1 mag drop in *W1* – *W2* colour during the burst, both of which are FUor-like. Source 812 lacks the same sampling of the other stars, with the photometry pre-2018 being unavailable in NEOWISE directly, and only three *W2* epochs being further visible in unTimely (Meisner et al. 2023). These do show a slow increase in brightness over a further 3 years before they too become non-detections. The 2.84 mag outburst has the shortest rise time in the sample, with an upper limit of 200 days. The final object, Source 1017, has the smallest outburst in the sample, but it novel for it having already returned to quiescence, meaning the outburst lasted just 6.5 years, very short for a FUor, but still longer than a traditional EXor. Given the similarity in shape, and the unusual colour behaviour, we cannot rule out that this is a luminous red novae (such as created by stellar mergers or planet engulfment, see Karambelkar et al. (2023)) although the pre-existing YSO classification does make this unlikely.

In addition to the sources detected from their outbursts in the MIR data, three further candidates were identified on the basis of outbursts observed in the UKIDSS UGPS (Lucas et al. 2008b) NIR images. All three were identified through searching for bursts of at least two magnitudes, wherein one UGPS epoch has a non-detection and the other had a minimum brightness of 15 mag (2 above the survey lower limit). Two of the three post-outburst light curves are displayed in figure 2, both of which display the traditional fading behaviour of post-outburst FUors. The third star is Source 1017, as seen in figure 1.

4.1.2 New EXor-like/Short Duration Eruptive YSOs

Thirteen stars in this sample displayed short term (i.e less than 3 years) variability, of greater than 1 magnitude in amplitude. These cuts should remove the majority of variables dominated by more commonplace accretion changes or sunspots, which are typically of lower amplitude (especially in the MIR), and shorter duration, see the results from YSOVAR (Morales-Calderón et al. 2011), or CSI 2264 (Cody et al. 2014). Stars that showed periodic dipping behaviour (like AA Tau) were also removed from this sample where obvious.

Some sources of note in this selection are discussed below:

- Source 1626 (Fig 4, bottom panel) has the largest single outburst of any of the short duration sources at 2.37 mag in *W1* (Table 4.1 gives the peak change across the whole light curve), which combines with a slight blueing of the colour of 0.28 in *W1* – *W2*. The single large burst lasts only for ~ 500 days, all of which is indicative of an EXor eruption.
- Source 185 has 4 quasi-periodic outbursts that each last for ~ 500 days (on of which is ongoing). We do not perceive the star to be ‘dipper’ because of the irregularity of the bursts (which could not be reliably fitted by normal period finding routines), which should be periodic if caused by extinction from orbiting material.
- Source 12 has 4 outbursts of > 1 mag in *W2*, which while repeating, are aperiodic. Unlike a typical EXor, Source 12 has redder-when-brighter colours, although given the high SED slope (1.03) this could be a result of reprocessing of more of the accretion luminosity into the MIR.
- Source 333 is of note from an additional long duration out-

² Based on observations collected at the German-Spanish Astronomical Center, Calar Alto, jointly operated by the Max-Planck-Institut für Astronomie Heidelberg and the Instituto de Astrofísica de Andalucía (CSIC).

Source Number	RA	Dec	Peak Amplitude /mag (W1)	Minimum W1 – W2 Colour	SED slope	Preliminary Classification
12*			2.004 ± 0.019	1.01	1.03	EXor-like
121*			1.848 ± 0.038	1.73	1.61	EXor-like
134			1.668 ± 0.008	1.494	0.34	LTE-SR
185			2.037 ± 0.07	3.05	-0.08	EXor-like
232			1.692 ± 0.01	1.54	0.44	EXor-like
236			1.432 ± 0.014	1.817	1.01	LTE-SR
257 [†]			3.279 ± 0.013	1.65	1.23	FUor-Like
294*			2.524 ± 0.02	0.77	1.2	FUor-Like
333			2.055 ± 0.011	1.33	0.4	EXor-like
352*			1.795 ± 0.02	2.82	1.52	EXor-like
387*			2.437 ± 0.097	1.97	0.27	EXor-like
441			1.674 ± 0.01	1.55	0.44	EXor-like
456			0.978 ± 0.016	0.7	0.16	EXor-like
591			2.354 ± 0.069	1.664	0.72	LTE-SR
625			3.371 ± 0.031	1.32	0.2	EXor-like
658			1.749 ± 0.011	1.26	0.27	LTE
769			2.817 ± 0.05	1.95	0.66	EXor-like
812			3.571 ± 0.046	1.93	1.54	FUor-Like
880			2.634 ± 0.03	1.27	0.22	LTE-SR
912			2.86 ± 0.036	2.732	0.88	LTE-SR
1017			2.313 ± 0.165	2.39	1.14	LTE
1048			3.981 ± 0.511	1.733	1.7	LTE-SR
1475			2.21 ± 0.053	2.81	1.19	FUor-Like
1562			3.081 ± 0.062	2.49	1.01	EXor-like
1626			3.081 ± 0.008	1.16	0.09	EXor-like
1769*			2.878 ± 0.008	2.27	1.15	LTE-SR
1884			1.438 ± 0.01	0.569	1.77	LTE-SR
1945			3.26 ± 0.041	1.961	0.77	LTE-SR
1991*			3.035 ± 0.056	2.827	0.96	LTE-SR
1999			4.606 ± 0.158	2.35	0.96	FUor-Like
2003			5.089 ± 0.017	1.67	1.01	FUor-Like

Table 1. List of sources for which an outburst was observed in the NEOWISE light curves. Sources marked as FUor-like have long duration outbursts with short rise times, and thus were well fitted by our model (Source 2003 is an exception to this fit, as its outburst is currently ongoing). An LTE classification covers the stars poorly fit by our FUor model, but that nonetheless have clear long-term eruptive behaviour, especially those with slow rise times (SR). Finally stars with mid to short duration outbursts are marked as EXor-like, for both stochastic and quasi-periodic eruptive sources. Source 257 (marked with a [†]) is included in the upcoming work of Contreras-Peña et al. (in prep), and will be discussed further there. Sources marked with an asterisk denote where the *Spitzer* detection is a blend between 2 detectable sources in UGPS.

burst of 1.55 mag in W1, which has been ongoing since April 2019, although it reached its peak after ~ 600 days. This burst was accompanied by a small reduction in the W1 – W2 colour, which was 2.13 at the start of the burst, but fell to 1.50 at the maximum (and has continued to fall even after the photometric maxima).

4.1.3 Source 232

Source 232 (also known as GPSV28 (Contreras Peña et al. (2014)) & IRAS 20226+4206), was also observed with a 1.0 mag outburst in *K* (in winter 2008), as part of the UKIDSS UGPS survey (included as Source 463 in Lucas et al. (2017)). Additionally it was observed twice further, as part of a pair of spectroscopic programmes, using Gemini/NIFS and Subaru/IRCS. These spectra can be seen in 5, which were acquired ~4 and ~6 years after the outburst respectively. The 2015 and 2017 spectra show notable differences in observed emission line ratios, wherein the 2015 spectrum has more prominent H₂ lines (S(1) and S(0)) than H I, and a clear Na I doublet. The implication being that flux is observed from the stellar photosphere, the inner accretion disk and outflows. By the 2017 spectrum, flux is dominated by the Brackett γ hydrogen recombination line, with a 3.98 ± 0.61 Å increase in measured equivalent width. Considering that this change implies an increase in the accretion rate, we speculate

that a higher proportion of the observed flux is from the hot inner-disk of the star, hence why emission lines associated with the photosphere are no longer detected. Whilst Source 232's initial outburst wasn't fully captured, a second 1.4 mag burst (in W1) was observed between the summers of 2021 and 2022, making clear that this star is EXor-like.

4.1.4 YSOs with Long-Term Accretion Trends

Eleven stars were identified with high-amplitude brightening trends with progressively bluer colours. These events continued for the >10 year duration of the NEOWISE observations, at a near-constant gradient. Whilst the observed variability could be attributed to continued accretion, it also resembles the pre-outburst light curve of the novel FUor Gaia17bpi (Hillenbrand et al. 2018), which would mean the behaviour could be attributed to a gravitational instability (GI) driven pile-up of material at the outer edge of the inner disk (see Bourdarot et al. (2023) & Cleaver et al. (2023) for simulations of both general FUor outbursts and the low-power Gaia17bpi-like ones respectively). This behaviour is also seen in the recently published flat-spectrum FUor WTP 10aaaouw (Tran et al. 2023), occurring in the years before the optically detected outburst. Outbursts with rise times on the order of a decade (as seen here) are predicted in the models of Borchert

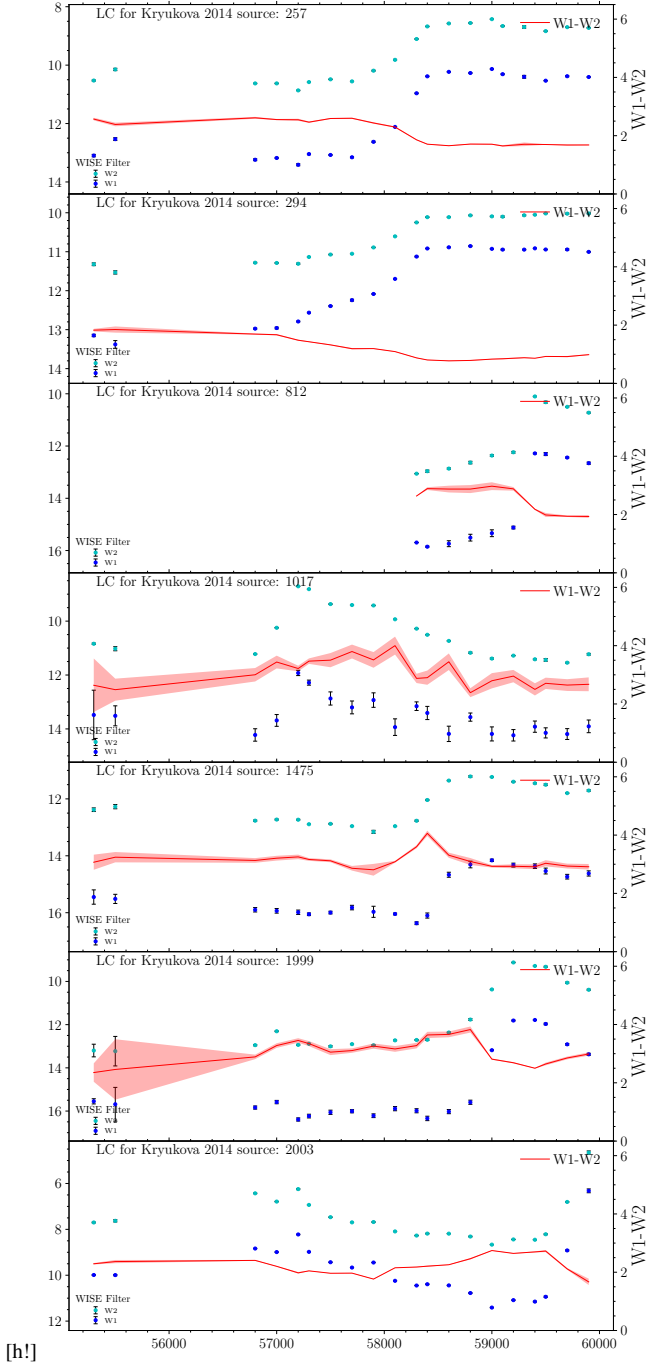


Figure 1. NEOWISE W1 & W2 light curves for 7 of the FUor candidates. Source 2003 is still in outburst, which could take its W1 amplitude to the largest ever observed in the MIR. Source 812 has more W2 epochs than displayed here, courtesy of the unTimely catalogue, although this data lacks much of the W1 epochs. The trends for W2 displayed a continued shallow rise from a magnitude of 16, at an MJD of 57340.

et al. (2022a), whose authors relate these to outbursts of lower accretion rate, but feeding from a reservoir of material at a larger rotation radius, on the order of 40-50 AU.

Figure 6 contains 7 of the 11 stars that fit this trend, (the other four are located in Figure A1). The group is fairly homogeneous with

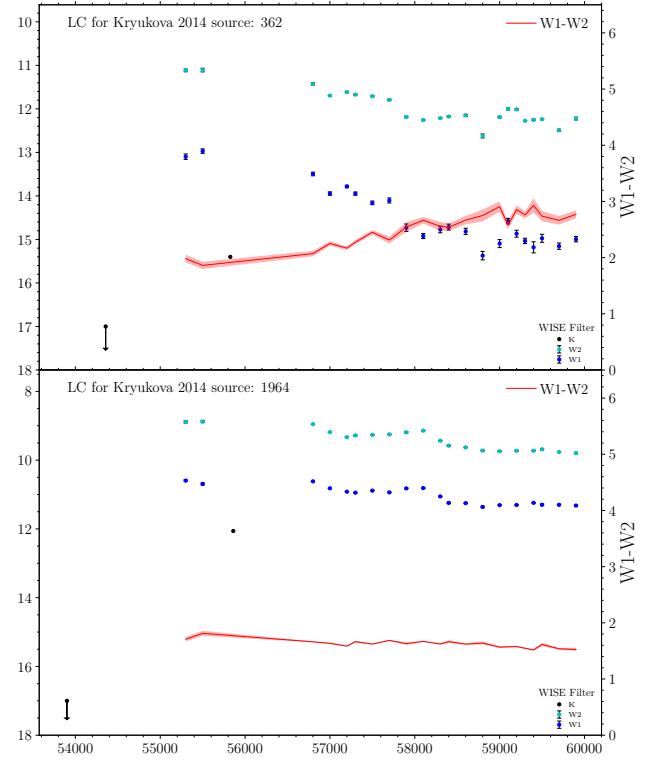


Figure 2. NEOWISE W1 & W2 light curves for Kryukova et al. (2014b) Sources 362 and 1964, which were detected through inspection of UGPS images. The black data points on the light curves represent the K -band magnitudes of the source, wherein the first data point is listed as an upper limit, as a result of being a non-detection.

regard to morphology, although certain stars (such as Sources 1769 and 1738) have other detected variability before the slower outbursts.

- Sources 1048 and 912 have two of the three highest amplitudes in the group, with $\Delta W1$ of 3.98 mag & 2.86 mag respectively. Both outbursts appear to have peaked, with 1048's lasting for ~ 8 years and 912's for ~ 5 years. The gradient of the rises are $\approx 0.50 \text{ mag yr}^{-1}$ and $\approx 0.70 \text{ mag yr}^{-1}$

- Source 1991 is similar in shape to those mentioned above, but has a much smaller drop in $W1 - W2$ colour, of ~ 0.27 mag. The photometric rise is of $\approx 0.41 \text{ mag yr}^{-1}$, continued monitoring of this star will determine if the last data point is indicative of the eruption finishing, or if it is simply a slight drop in luminosity, as seen in sources 1945 and 134.

- Source 1884 has the second lowest amplitude of the stars in this group at 1.44 mag (with a gradient of $\approx 0.36 \text{ mag yr}^{-1}$), but this is combined with the lowest quiescent $W1 - W2$ colours (between 1.11 mag and 0.56 mag).

Continued photometric monitoring of all these sources will be of importance in understanding the frequency with which behaviour of this form leads to FU Ori-like eruptions. In turn this could provide the ability to monitor FUor systems before outburst, possibly discovering the mechanism that drives the eruption in these embedded systems.

4.2 Cygnus-X YSOs without [24] detections, from SPICY

We find 37 EV candidates (see Table 2) from 402 stars with > 1 magnitude variance in either W1 or W2, with the vast majority of

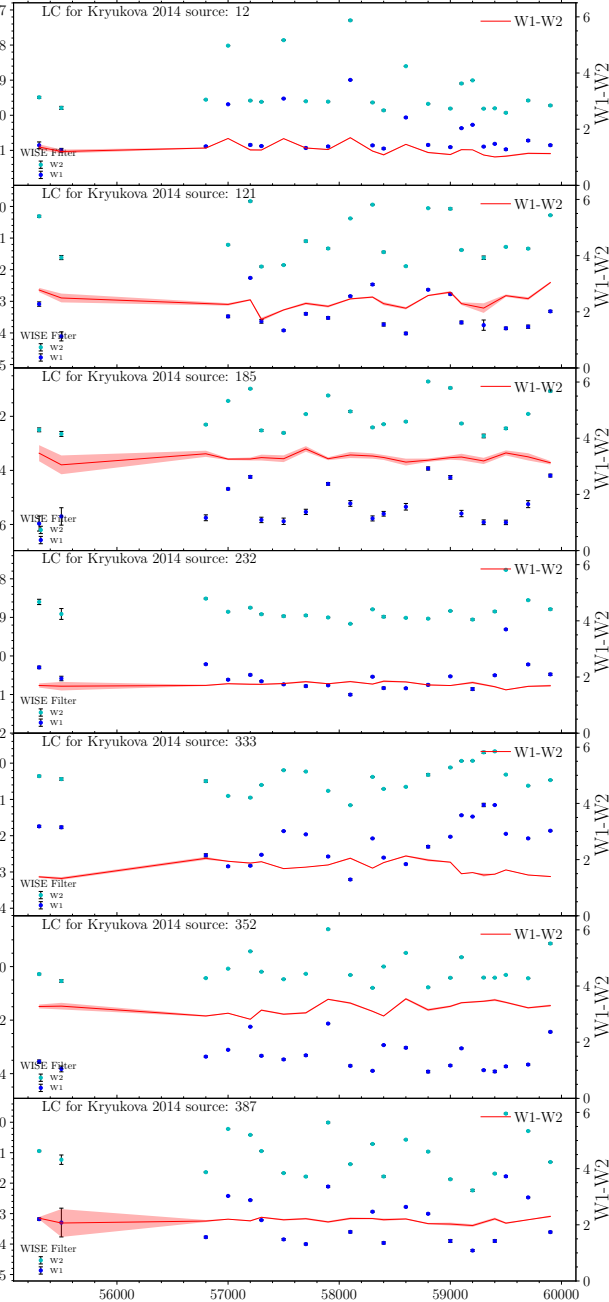


Figure 3. NEOWISE W1 & W2 light curves for the first 7 EXor candidates in the sample.

variables showing clear ‘dipper’-like extinction behaviour. Of the EVs 25 are class II YSOs (with $K - I_4$ SED slopes < -0.3), 4 are Class III YSOs, 7 are FS sources, and 1 is considered uncertain, although its average WISE colours ($W1 - W2 = 1.66$) are comparable to the bluer Class I sources from section 4.1.2. Across the sample we note the variation in the $W1 - W2$ colour during outburst, wherein 23/37 stars show redder colours when brighter.

4.2.1 New FUor-like/Long Duration Eruptive YSOs

The outburst detection code discussed in section 2 located 3 stars with a shape comparable to that of an archetypal FUor (SPICY

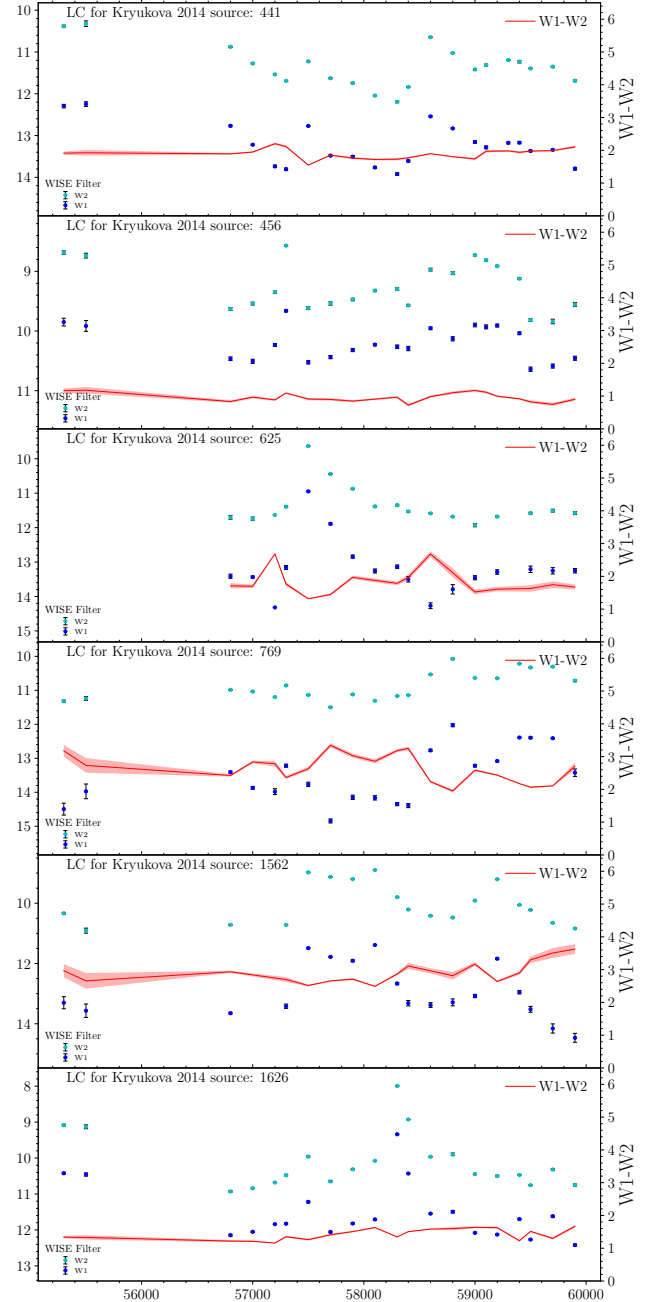


Figure 4. NEOWISE W1 & W2 light curves for the second 6 EXor candidates in the sample.

108461, 109060 & 114590), although all have peak amplitudes of < 2 magnitudes (see figure 7). The MIR colour behaviour is different for each star, although each star is also of a different SED class, which may partially explain the discrepancy. These low amplitudes are not unexpected in the general sense, with models for YSOs with already enhanced accretion rates having lower outburst amplitudes, as seen in Hillenbrand & Rodriguez (2022) (Figure 1). It cannot be ruled out however that these three stars may be emission line sources, more akin to a long-duration EXor, than a true FUor.

SPICY 111892 has been previously identified as a eruptive variable candidate in UGPS in both Contreras Peña et al. (2014); Lucas et al. (2017) (as GPSV64). It displayed a 1.5 mag increase in brightness

Table 2. Table for the 37 EV candidates found in the 402 YSOs with 1+ mag variability. The distances between WISE and *Spitzer* centroids were compared in order to locate any possible blended sources. The colour behaviour column notes how the $W1 - W2$ colour changes during the eruptive portions of the light-curve: BWB means the source is bluer-when-brighter (much like traditional EXors), RWB indicates redder-when-brighter behaviour, and "Varied" notes stars whose colour behaviour changes over the total duration of the light curve.

SPICY ID	RA	Dec	Peak Amplitude /mag (W1)	Minimum W1 – W2 Colour	Colour Behaviour	SED Class
107699			1.025 ± 0.010	0.321	RWB	Class II
107742			1.054 ± 0.010	1.338	BWB	Class II
107855			0.969 ± 0.008	0.550	No Change	Class II
108461			1.959 ± 0.031	0.679	BWB	Class II
108504			1.125 ± 0.013	0.441	RWB	Class II
108553			0.855 ± 0.017	0.698	RWB	Class II
108835			1.338 ± 0.046	0.786	BWB	Class II
109025			0.875 ± 0.006	0.103	RWB	Class III
109060			1.027 ± 0.014	-0.007	RWB	Class III
109259			1.233 ± 0.014	1.091	BWB	Class II
109392			1.904 ± 0.015	0.332	RWB	Class II
109705			4.121 ± 0.021	1.171	BWB	FS
109973			0.817 ± 0.021	0.345	RWB	Class II
110521			0.836 ± 0.007	0.157	RWB	Class II
110601			0.931 ± 0.010	0.416	RWB	Class III
110991			1.315 ± 0.008	0.713	RWB	Class II
111048			1.677 ± 0.011	0.025	RWB	Class II
111336			1.522 ± 0.036	-0.124	RWB	Class II
111413			1.165 ± 0.023	0.443	RWB	FS
111739			1.810 ± 0.067	1.346	BWB	?
111836			1.125 ± 0.014	0.821	RWB	Class II
111892			0.876 ± 0.008	1.050	BWB	FS
112458			0.616 ± 0.057	-0.420	RWB	Class II
112533			1.561 ± 0.018	0.007	RWB	Class II
112884			0.614 ± 0.011	0.180	RWB	Class II
112979			1.201 ± 0.006	0.442	RWB	Class II
113094			1.672 ± 0.001	0.902	BWB	Class II
113145			1.489 ± 0.015	0.643	RWB	Class II
113564			1.550 ± 0.016	0.609	Varied	Class II
113803			0.904 ± 0.009	0.166	RWB	Class III
113865			1.043 ± 0.049	-0.100	Varied	FS
113929			0.940 ± 0.005	0.441	RWB	Class II
114037			1.001 ± 0.051	-0.018	Varied	Class II
114471			1.371 ± 0.015	0.417	BWB	Class II
114590			1.603 ± 0.034	0.542	RWB	FS
115546			0.662 ± 0.023	0.732	RWB	FS
115613			1.158 ± 0.010	0.777	No Change	FS

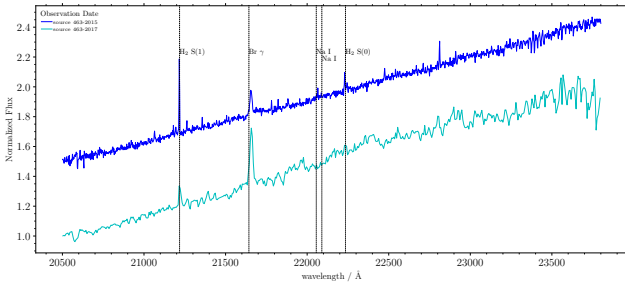


Figure 5. K and K' spectra for Source 232, taken in 2015 and 2017. note the absence of photospheric lines from sodium in the 2017 spectrum.

between 2006 and 2009, which would be low for a FUor if this is the true amplitude. That is not the whole picture however, as the non-detection in earlier 2MASS images implies a longer rise time, and a higher amplitude. Given that actual lower limits for 2MASS vary frame by frame, the value for the image in which SPICY

111892 resides is calculated at 16.0. This was found by running the photutils method called ImageDepth. This takes the zero-point for the instrument, and a selection of magnitudes of stars in the image, and computes the lowest detectable flux for a given precision in sigma (quoted here are 3σ values) for a large number of randomly placed apertures. Thus the total ΔK amplitude has a lower limit of 4.0 mag, over a duration of ~ 4000 days. A follow up spectrum was obtained in the winter of 2014 (Fig 8) with Gemini/NIFS, which shows the mostly featureless red continuum and broad CO bandheads often associated with FUor spectra (the large emission line at $2.292\mu\text{m}$ is likely spurious, as it had appeared in a large number of other YSOs in the same set of observations).

4.2.2 New EXor-like/Short Duration Eruptive YSOs

Of the 37 EV candidates in this group 89% (33) have short duration EXor-like outburst events. given the known diversity of these systems, it comes as little surprise that we see significant variation in the observed light curve morphologies. We include four stars in Figure

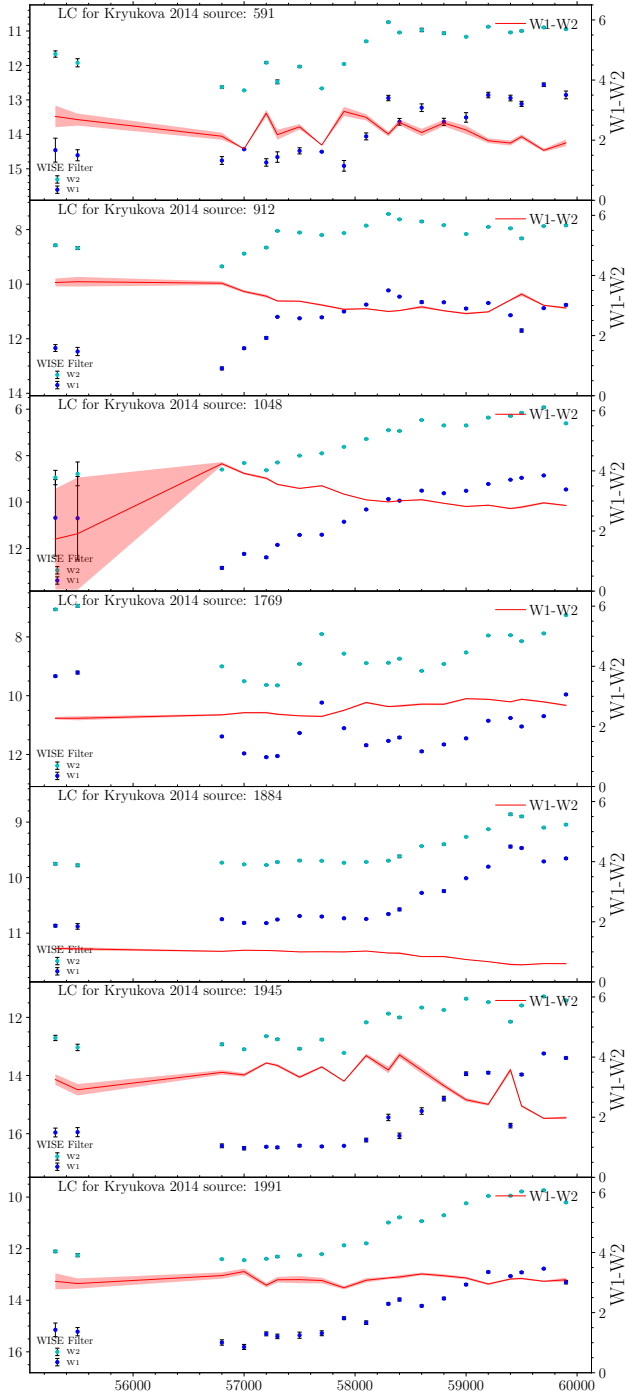


Figure 6. NEOWISE W1 & W2 light curves for a selection of the slowly brightening sources (others will be available in the appendix). Of some doubt is source 1769, which has ALLWISE data points at a comparable magnitude to the current brightness level of the source, and lacks the similar bluer when brighter colours of the other stars in the group.

9 that illustrate the variety (the rest can be seen in Appendix B). SPICY 113094 displays quasi-periodic behaviour at a roughly 550 day period³, with each burst of up to 1.6 mag and bluer colours at this point. This is characteristic of stars such as SPICY 116663 (Kuhn

³ fitted using the *astropy* *LombScargle* function.

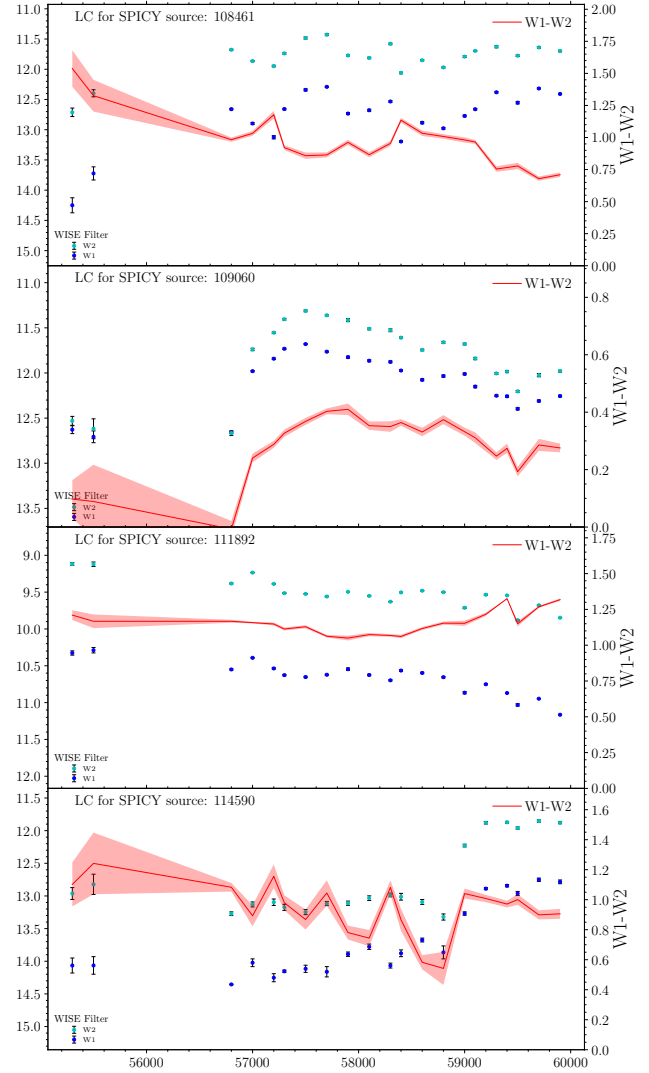


Figure 7. NEOWISE W1 & W2 light curves for 3 FUor candidates from the SPICY selected Class II/Flat-spectrum sources. The outbursts are of significantly lower amplitude than those found in the [24] micron detected sample, but are in-line with the MIR amplitudes seen in many literature objects. Source 111892 is included here as a FUor-like star with an outburst first detected in 2MASS, and again in UGPS.

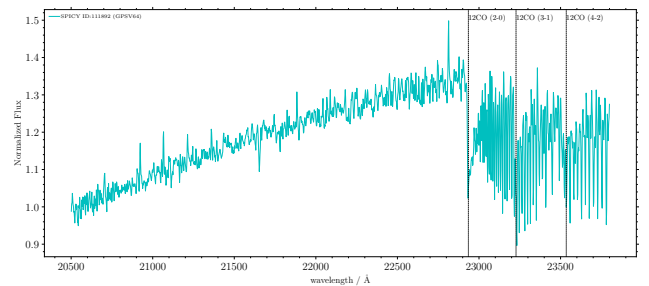


Figure 8. Gemini/NIFS spectrum for SPICY 111892 (GPSV64 from Contreras Peña et al. (2014)). The spectrum is obviously FUor-like, with a featureless red continuum, and strong 12CO absorption lines from the star's mid-planar region.

et al. 2021), albeit with a longer period than that example. SPICY 110521 shows repeating burst behaviour, although without any clear periodicity, effectively ruling out AA Tau-like occultation by dust. With outbursts of over one magnitude and colours that redden with increases in luminosity, it is however unlike the typically expected behaviour of classical EXors, as described by Lorenzetti et al. (2012), wherein colours are often expected to become bluer during outburst. The behaviour seen in SPICY 110521 is commonly seen in this sample: 20 of 33 (60.6%) short duration (EXor-like) eruptives are redder in outburst. [zzz DISCUSS FURTHER? zzz]. SPICY 111336 also displays aperiodic, repetitive outbursts, but these are of differing amplitude, in contrast to many of the other repeating sources. The amplitudes in W2 range from ~ 0.7 mag to ~ 1.5 mag, although they are of a similar ~ 400 day duration (the duration is an upper limit owing to the wide sampling of NEOWISE). The final EXor-like star to be discussed will be SPICY 112533, which is the most unusual star in this sample of older YSOs. Seemingly there are two components to the light curve, with a long term fading trend, which is separate to 5 detected outbursts each of between ~ 0.8 & 1.0 mag and ~ 1.0 & 2.0 mag in W1 & W2 respectively. Of additional note is the single outburst of at least 900 days (between 2016 and 2018) which bears little resemblance to other EXor-like bursts, owing to the comparatively short cooling timescale as compared to the rise time.

Overall the sample of short-term variables is slightly biased towards sources with repetitive outburst behaviour, as is the case for 60.6% (20/33) of the sample. Whilst none of these are obviously truly periodic, 5 of the stars display bursts which can likely be termed quasi-periodic, with timescales of over 400 days (the lowest that can be reliably identified with NEOWISE given the sampling).

5 DISCUSSIONS

5.1 Comparison of Embedded FUor Candidates to Classical FUors

Given the comparatively low number of known FUor like stars, our discovery of up to 16 (although likely less) new members within a single SFR warrants additional investigation. Given that our main sample was of the most embedded EVs within Cygnus-X, comparing their MIR behaviour to that of FUors discovered via a 'traditional' optical outburst could reveal differences between the two populations.

most classical (NIR/Optical detected) FUors show a negative correlation between their W2 amplitudes and $W1 - W2$ colours (Fig 10 - blue points), whereas this does not hold true for the Eruptives in our sample (Fig 10 - red and cyan points). The embedded EVs seem to hold a slight positive correlation, although all still show the normal bluer-when-brighter colour behaviour during the outburst, similar to normal FUors. The figure also places the slowly-rising eruptive variables amongst the FUor candidates, giving further weight to our hypothesis that these sources are YSOs that are building up to a FUor-like outburst (which may be optically detectable), in a similar vein to Gaia18bpi or WTP 10aaaouw. The reasoning for inversion of the colour/amplitude relation for the embedded sources is not yet fully clear, although a thicker envelope (and thus redder quiescent colours) might imply that we are seeing greater reprocessing of the accretion luminosity into the MIR, inflating the observed amplitude.

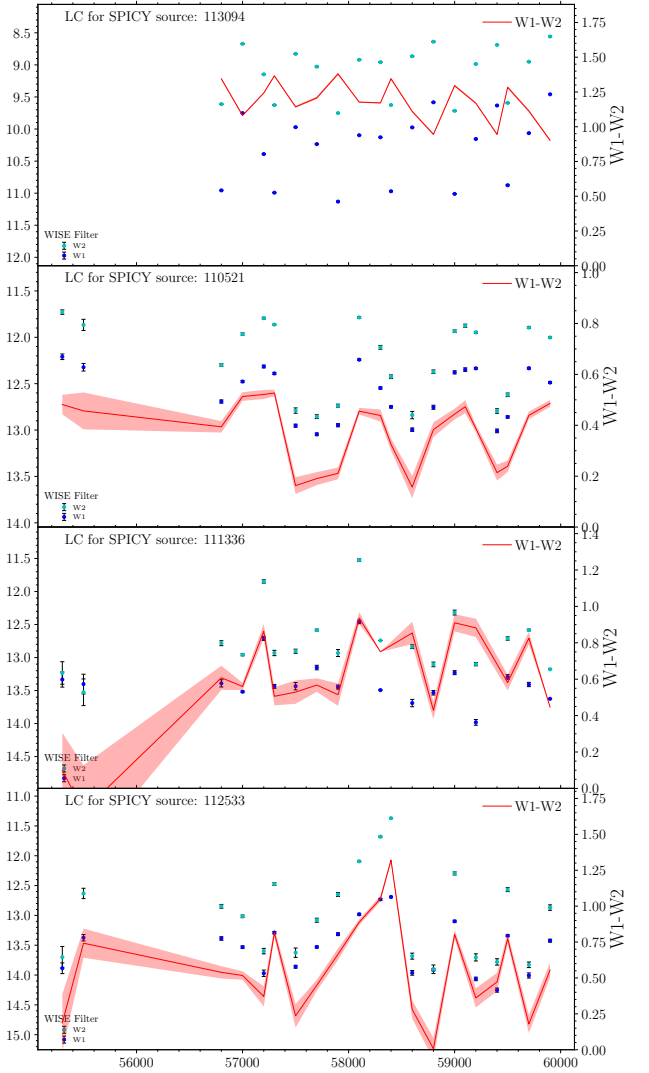


Figure 9. NEOWISE W1 & W2 light curves for four EXor candidate eruptive variables. These are selected because they demonstrate a wide range of behaviours and outburst durations. Of particular note is Source 112533, which had periodic small outbursts after a much larger, long duration event.

5.2 Comparing the Rates of Eruptive Behaviour in Cygnus-X Between Embedded and Non-Embedded Sources

By having a control sample of known YSOs, we can compare both the rates and amplitudes of eruptive variability for our embedded YSOs to those of the older sources within Cygnus-X. The comparison between number density and amplitude for both of our samples can be seen in Figure 11, with the Class I sources in the left panel, and the Class II and flat-spectrum sources in the right. It can be clearly seen that the embedded sources have a higher number density of high amplitude variables than the older sources. This is most evident looking at the percentage of stars with amplitudes > 1 mag, with 22.46% of stars reaching this threshold in W1 for the embedded sample, but just 4.94% for the FS/class II stars from SPICY. It must be noted that only a proportion of each of these variables are likely eruptive, with large numbers of AA Tau-like 'dippers', short-term (possibly spurious) variables and stars on long-term fading trends. A proportion of this latter group also may well be eruptive YSOs, wherein a large outburst has happened outside of our window of

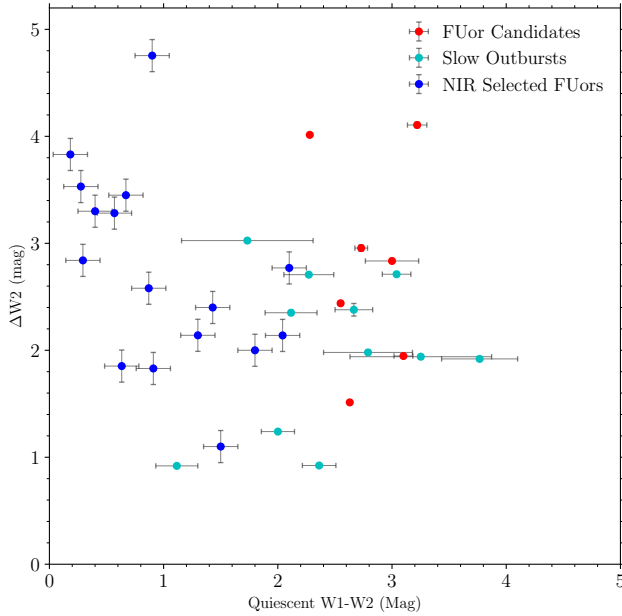


Figure 10. W2 amplitude against median W1-W2 colours for the stars discussed in section 4.1. Key differences exist in this sample versus the catalogue of eruptive YSOs of Guo et al. (subm.), wherein the majority of FUors in those authors’ sample exist on the upper left of the diagram, whereas ours are in the upper right.

observation, and we are now witnessing the post-outburst cooling phase (this will be investigated in Contreras-Peña et al. In Prep.). The statistics for solely obvious eruptive sources do continue the trend of high amplitude variability being more common for embedded sources however, because both samples have an 10% EV fraction within the sample of stars with amplitudes greater than 1 mag (9.5% (33/348) for the Class I sample and 9.2% (37/402) for the Class II and FS stars). To test the significance of these results, we performed a Wilcoxon-Mann-Whitney U test, between both samples. Because the sample of FS and Class II sources is substantially larger than that of the embedded stars, we instead perform our WMW-U test on two equal sized samples drawn from distributions defined by a Gaussian kernel density estimation (fitted to all four histograms in Figure 11), both of these routines are carried out in *Python*, using the relevant routines in *scipy.stats*. This test produced an average p-value of 3.46% over 10000 iterations, and thus we can reject our null hypothesis that these two samples were drawn from the same distribution.

From the perspective of stellar evolution the above result is within expectation, as younger systems will have a larger reservoir of material with which to accrete from, and is possibly more unlikely to become unstable, leading to GI driven outbursts. Hence searching for EVs in younger systems specifically should lead to a larger samples, especially of the rarer FU Ori-type objects. This falls into the long held view that longer duration outbursts happen in younger systems (Hartmann & Kenyon 1996a), given the long average length of FUor events. The differing morphologies of some of our long duration outbursts also fit in to the ideas of Quanz et al. (2007), which describe a possible evolutionary sequence for FUors, based upon their MIR features. The above point makes a strong case for follow-up spectroscopy at both near and mid-infrared wavelengths. We also note that the EXor-like stars in our embedded sample do seem to have longer outbursts on average than the usual order-of-months timescales of the

these objects classically. Although given the fairly sparse sampling of NEOWISE we cannot rule out a significant selection bias.

6 SUMMARY

In this work we have presented 70 MIR-selected eruptive variable YSOs on the basis of their behaviour in NEOWISE long-duration light curves. Amongst these are 12 candidate FUors of a more classical type, and an additional 10 YSOs with slower brightening phases, which may also be FUor-like in nature. We also locate a large number of EXors within both samples carried out, with 13 embedded class I YSOs and 32 flat-spectrum or class II stars. We note the greater numbers of detected high amplitude (and eruptive) variables found within our sample of embedded YSOs, which suggests that large accretion rate changes are common for younger protostars. This is especially true for the FUor type EVs, of which we have identified between up to 16 candidate members, a number of which are of a novel, slow-rising character. Given the similarities between these objects and the pre-outburst light curves of several novel FUors, these ‘slow-risers’ might be further examples of FUors that outburst at earlier times in redder wavelengths.

Given the possible new population of eruptive young stars, follow-up spectroscopy and photometry is planned for those stars still at a state of high accretion. This may unveil any differences in accretion behaviour and disk/wind structure between the heavily embedded EVs and the traditional optical/NIR selected stars.

ACKNOWLEDGEMENTS

We thank Calar Alto Observatory for allocation of director’s discretionary time to this programme.

ZG is supported by the ANID FONDECYT Postdoctoral program No. 3220029. ZG acknowledge support by ANID, – Millennium Science Initiative Program – NCN19_171.

DATA AVAILABILITY

The inclusion of a Data Availability Statement is a requirement for articles published in MNRAS. Data Availability Statements provide a standardised format for readers to understand the availability of data underlying the research results described in the article. The statement may refer to original data generated in the course of the study or to third-party data analysed in the article. The statement should describe and provide means of access, where possible, by linking to the data or providing the required accession numbers for the relevant databases or DOIs.

REFERENCES

- Audard M., et al., 2014, Technical report, Episodic Accretion in Young Stars, <https://arxiv.org/pdf/1401.3368.pdf>. (arXiv:1401.3368v1), <https://arxiv.org/pdf/1401.3368.pdf>
- Barentsen G., et al., 2014, *MNRAS*, **444**, 3230
- Bell K. R., Lin D. N. C., 1994, *ApJ*, **427**, 987
- Borchert E. M. A., Price D. J., Pinte C., Cuello N., 2022a, *MNRAS*, **510**, L37
- Borchert E. M. A., Price D. J., Pinte C., Cuello N., 2022b, *MNRAS*, **517**, 4436
- Bourdarot G., et al., 2023, *A&A*, **676**, A124
- Clarke C., Lodato G., Melnikov S. Y., Ibrahimov M. A., 2005, *MNRAS*, **361**, 942

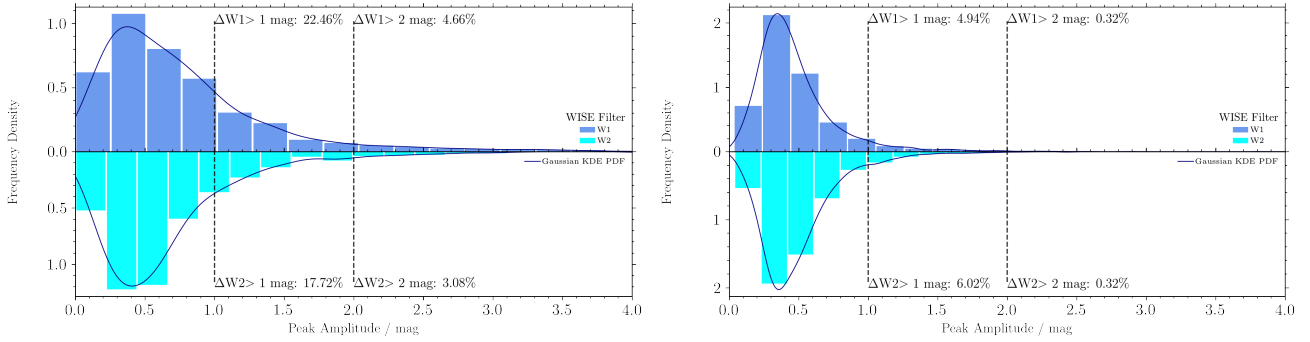


Figure 11. Histograms displaying peak amplitudes in W1 & W2 for both of the two samples discussed in Section 4. Each individual histogram is presented with a probability distribution function, created by running a gaussian kernel density estimation using a routine included in *scipy*. Note that the sources with a MIPS [24] detection from the Kryukova et al. (2014b) sample have a much broader range of amplitudes.

Cleaver J., Hartmann L., Bae J., 2023, *MNRAS*, **523**, 5522
 Cody A. M., et al., 2014, *AJ*, **147**, 82
 Connelley M. S., Reipurth B., 2018, *The Astrophysical Journal*, **861**, 145
 Contreras Peña C. E., 2015, PhD thesis, University of Hertfordshire, UK
 Contreras Peña C., et al., 2014, *MNRAS*, **439**, 1829
 Contreras Peña C., et al., 2017, *MNRAS*, **465**, 3011
 Contreras Peña C., et al., 2017, *Monthly Notices of the Royal Astronomical Society*, **465**, 3039
 Cuello N., et al., 2019, *MNRAS*, **483**, 4114
 Fischer W. J., Hillenbrand L. A., Herczeg G. J., Johnstone D., Kóspál Á., Dunham M. M., 2022, *arXiv e-prints*, p. [arXiv:2203.11257](#)
 Guo Z., et al., 2021, *MNRAS*, **504**, 830
 Guo Z., et al., 2022, *MNRAS*, **513**, 1015
 Hartmann L., Kenyon S. J., 1996a, *ARA&A*, **34**, 207
 Hartmann L., Kenyon S. J., 1996b, *Annual Review of Astronomy and Astrophysics*, **34**, 207
 Hartmann L., Zhu Z., Calvet N., 2011, *arXiv e-prints*, p. [arXiv:1106.3343](#)
 Hillenbrand L. A., Rodríguez A. C., 2022, *Research Notes of the American Astronomical Society*, **6**, 6
 Hillenbrand L. A., et al., 2018, *ApJ*, **869**, 146
 Hora J., et al., 2007, A Spitzer Legacy Survey of the Cygnus-X Complex, Spitzer Proposal ID #40184
 Karambelkar V. R., et al., 2023, *ApJ*, **948**, 137
 Kovács Z., Mall U., Bizenberger P., Baumeister H., Röser H.-J., 2004, in Garnett J. D., Beletic J. W., eds, *Society of Photo-Optical Instrumentation Engineers (SPIE) Conference Series Vol. 5499, Optical and Infrared Detectors for Astronomy*. pp 432–441, [doi:10.1117/12.551194](#)
 Kratter K., Lodato G., 2016, *ARA&A*, **54**, 271
 Kryukova E., et al., 2014a, *AJ*, **148**, 11
 Kryukova E., et al., 2014b, *The Astronomical Journal*, **148**, 11
 Kuhn M. A., de Souza R. S., Krone-Martins A., Castro-Ginard A., Ishida E. O., Povich M. S., Hillenbrand L. A., COIN Collaboration 2021, *ApJS*, **254**, 33
 Kuhn M. A., Benjamin R. A., Ishida E. O., de Souza R. S., Peloton J., Veneri M. D., 2023, *Research Notes of the American Astronomical Society*, **7**, 57
 Liu H., et al., 2022, *ApJ*, **936**, 152
 Lorenzetti D., et al., 2012, *The Astrophysical Journal*, **749**, 188
 Lucas P. W., et al., 2008a, *MNRAS*, **391**, 136
 Lucas P. W., et al., 2008b, *Monthly Notices of the Royal Astronomical Society*, **391**, 136
 Lucas P. W., et al., 2017, *Monthly Notices of the Royal Astronomical Society*, **472**, 2990
 Mainzer A., et al., 2014, *ApJ*, **792**, 30
 Manara C. F., Ansdell M., Rosotti G. P., Hughes A. M., Armitage P. J., Lodato G., Williams J. P., 2022, *arXiv e-prints*, p. [arXiv:2203.09930](#)
 Meisner A. M., Caselden D., Schlafly E. F., Kiwy F., 2023, *AJ*, **165**, 36
 Minniti D., et al., 2010, *New Astronomy*, **15**, 433
 Morales-Calderón M., et al., 2011, *ApJ*, **733**, 50

Quanz S. P., Henning T., Bouwman J., van Boekel R., Juhász A., Linz H., Pontoppidan K. M., Lahuis F., 2007, *ApJ*, **668**, 359
 Sandell G., Weintraub D. A., 2001, *ApJS*, **134**, 115
 Scholz A., Froebrich D., Wood K., 2013, *MNRAS*, **430**, 2910
 Skrutskie M. F., et al., 2006, *AJ*, **131**, 1163
 Tran V., De K., Hillenbrand L., 2023, *arXiv e-prints*, p. [arXiv:2310.10832](#)
 Vorobyov E. I., Basu S., 2010, *ApJ*, **719**, 1896
 Wright E. L., et al., 2010, *AJ*, **140**, 1868
 Zhu Z., Hartmann L., Gammie C., McKinney J. C., 2009, *ApJ*, **701**, 620

APPENDIX A: ADDITIONAL LIGHT CURVES FROM THE EMBEDDED YSO SAMPLE

Listed in this section are the light curves from the stars not mentioned directly in the text.

APPENDIX B: LIGHT CURVES FOR HIGH AMPLITUDE VARIABLE YSOS FROM SPICY

Listed here are the NEOWISE MIR light curves for the EXor candidates discussed in section 4.2.

This paper has been typeset from a \LaTeX file prepared by the author.

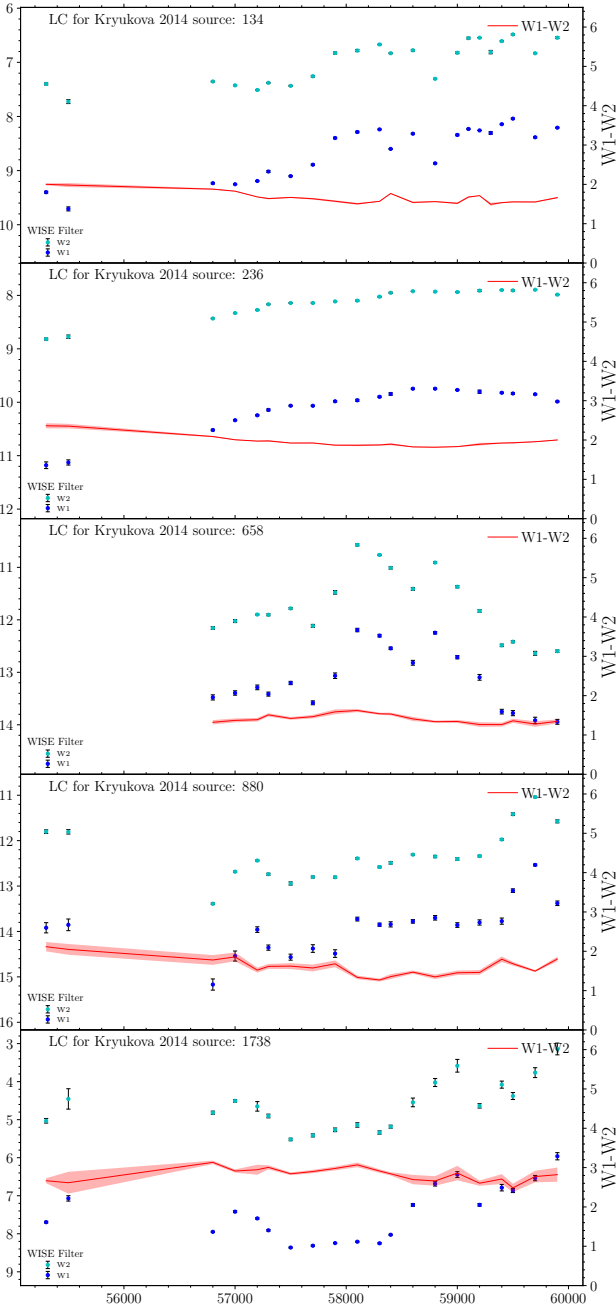


Figure A1. NEOWISE W1 & W2 light curves for the five long duration outbursts not discussed in the main text.

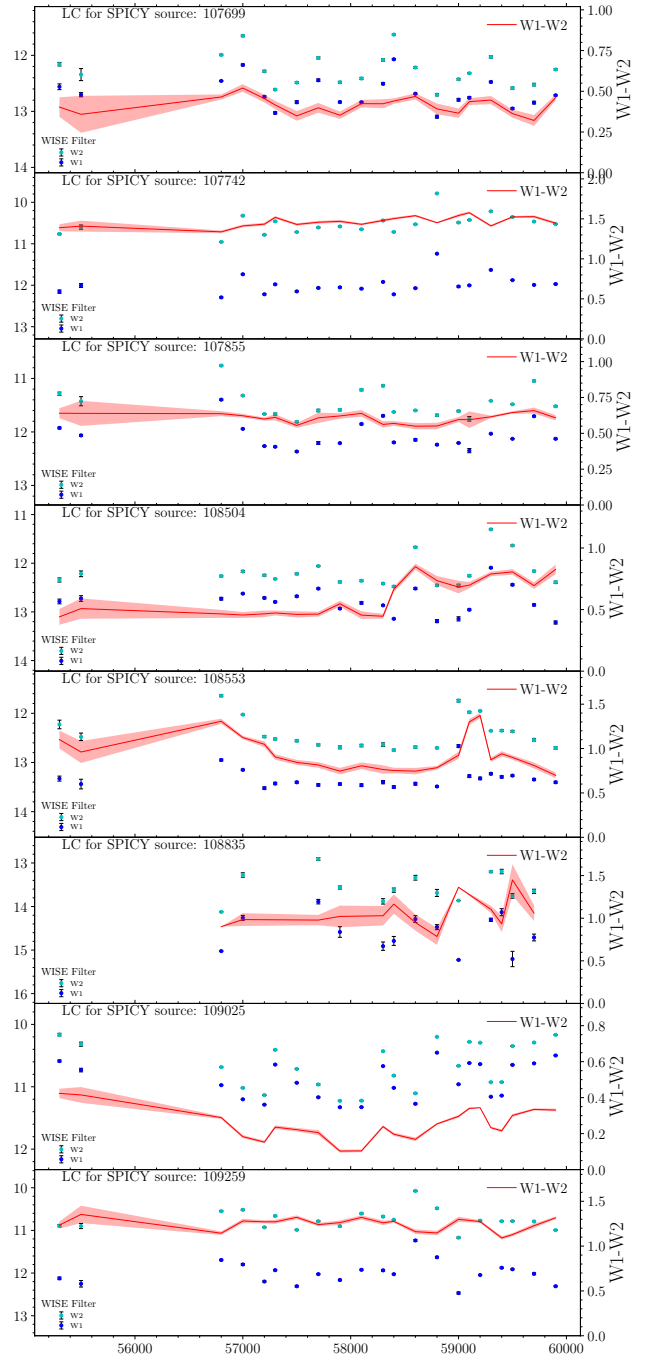


Figure B1. NEOWISE W1 & W2 light curves for the EXor candidates in the SPICY selected sample.

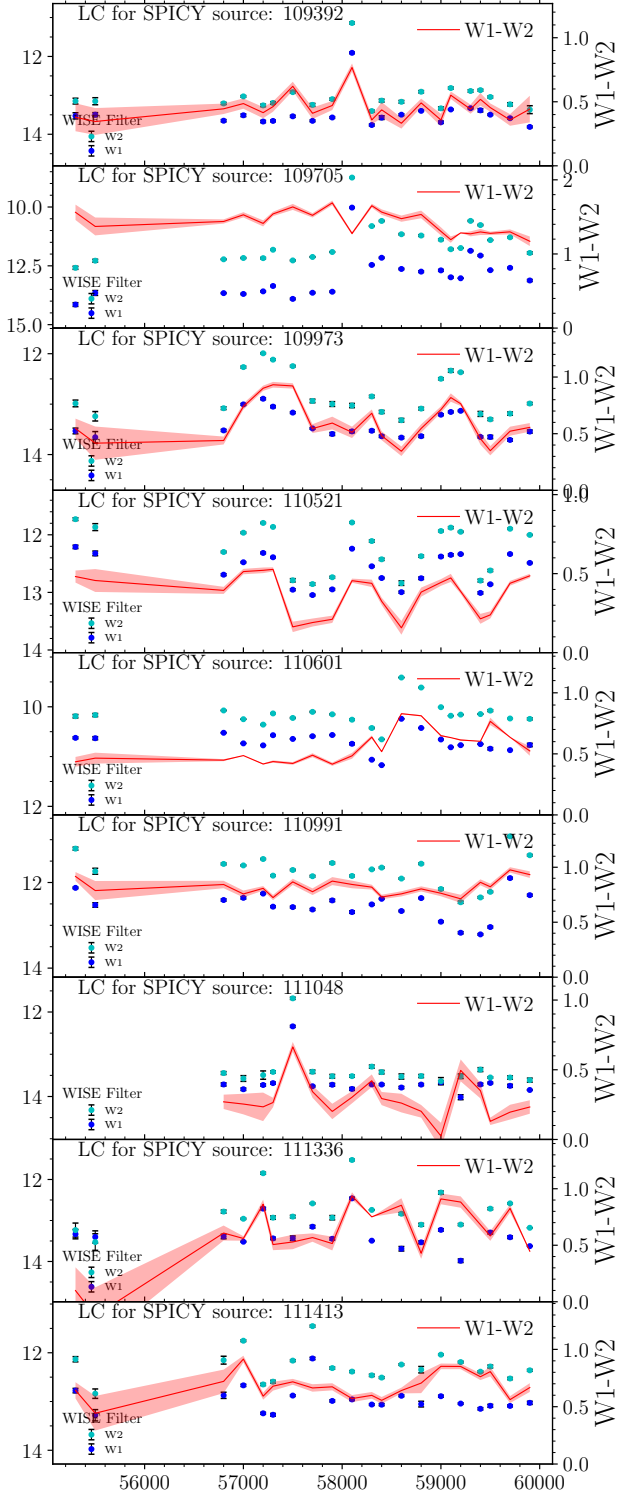


Figure B2. NEOWISE W1 & W2 light curves for the EXor candidates in the SPICY selected sample.

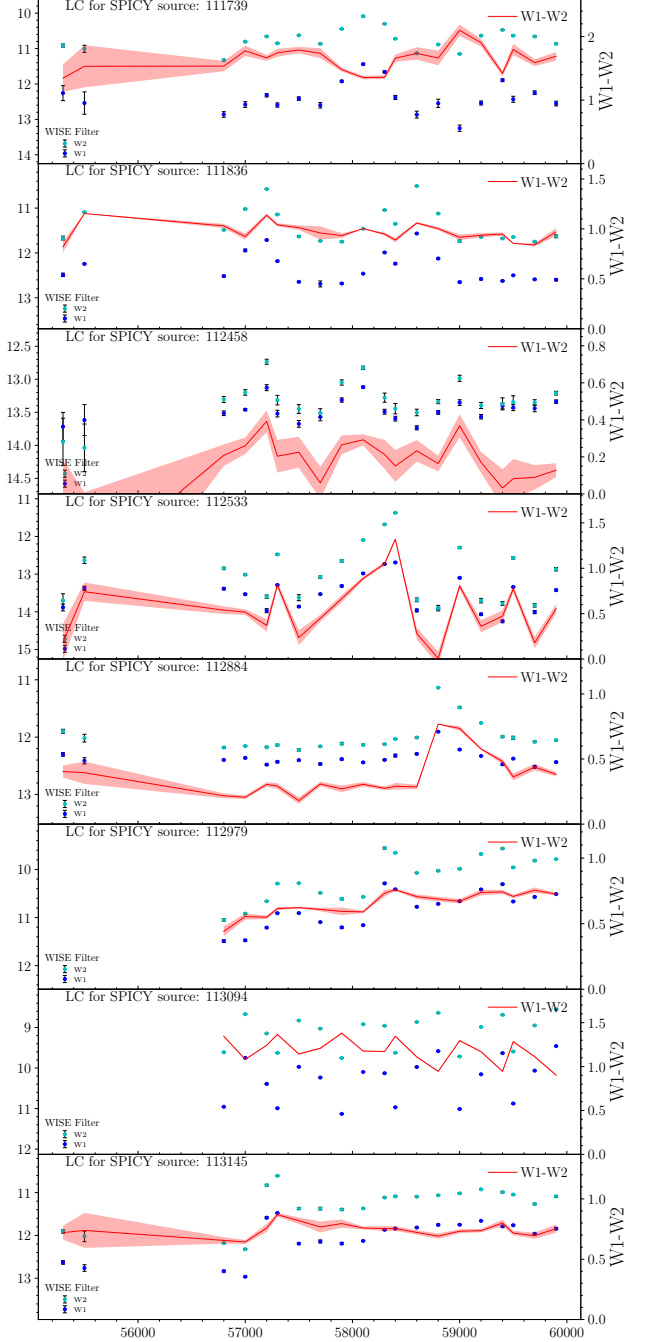


Figure B3. NEOWISE W1 & W2 light curves for the EXor candidates in the SPICY selected sample.

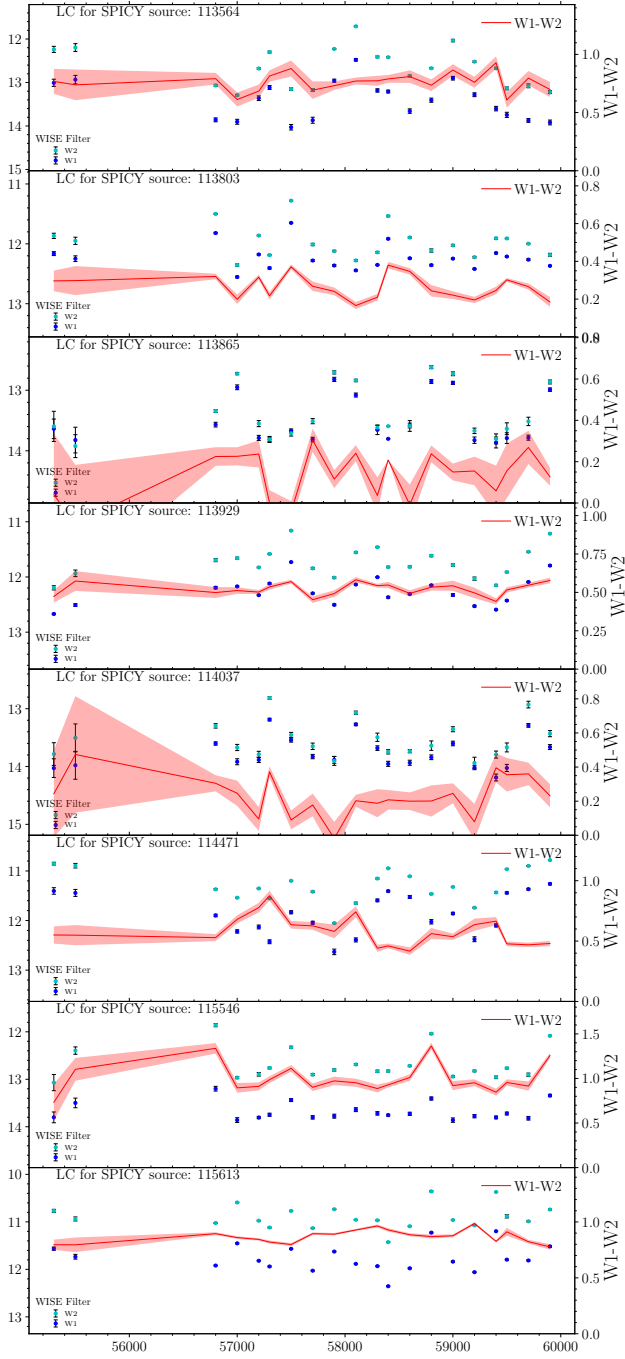


Figure B4. NEOWISE W1 & W2 light curves for the EXor candidates in the SPICY selected sample.